Journal of Alloys and Compounds 526 (2012) 98–102

Contents lists available at SciVerse ScienceDirect

Journal of Alloys and Compounds

journal homepage: www.elsevier.com/locate/jallcom

Electron magnetic resonance study of monovalent Na doping in $Pr_{0.6}Sr_{0.4-x}Na_xMnO_3$ manganites

Rachid Thaljaoui[a,b,c], Wahiba Boujelben[a,*], Marek Pękała[c], Jadwiga Szydłowska[c], Abdelwaheb Cheikhrouhou[a,d]

[a] Laboratoire de Physique des Matériaux, Faculté des Sciences de Sfax, Université de Sfax, B.P. 1171, 3000 Sfax, Tunisia
[b] Faculty of Physics, Warsaw University of Technology, Koszykowa 75, 00-662 Warsaw, Poland
[c] Department of Chemistry, University of Warsaw, Al. Zwirki i Wigury 101, 02-089, Poland
[d] Institut NEEL, CNRS, B.P.166, 38042 Grenoble Cedex 9, France

ARTICLE INFO

Article history:
Received 9 January 2012
Received in revised form 9 February 2012
Accepted 13 February 2012
Available online xxx

Keywords:
Manganites
Ferromagnetic and electron paramagnetic resonance
Polaron hopping
Magnetic interactions

ABSTRACT

Effect of monovalent Na doping on the magnetic properties is studied in $Pr_{0.6}Sr_{0.4-x}Na_xMnO_3$ system ($x = 0$, 0.05) using X-band electron magnetic resonance and magnetization measurements. Temperature variation of magnetic resonance spectra of doped and undoped manganites is analyzed for paramagnetic and ferromagnetic states and compared to similar systems. In paramagnetic phase the magnetic susceptibility proportional to resonance signal intensity is found to obey the Curie–Weiss law. The effective magnetic moment becomes smaller in doped manganite. The paramagnetic Curie temperature derived from signal intensity equals to 312 and 306 K for the undoped and doped manganites, respectively, and is close to values obtained from magnetization variation in paramagnetic phase. The activation energy determined using the adiabatic small polaron hopping model is higher for the undoped than the doped manganite, which proves that the Na doping slightly reduces the Mn^{3+}/Mn^{4+} double exchange interactions.

1. Introduction

Doped perovskite manganites with general formula $A_{1-x}R_xMnO_3$ (A = rare-earth cation, R = alkaline earth cation) have attracted much attention for interesting physical properties around the phase transition temperature T_C and because of possible applications [1–4]. The heterovalent substitution of A for R leads to a mixed valence Mn^{3+}/Mn^{4+} state and induces a transition from paramagnetic-insulator to a ferromagnetic-metallic phase. This in turn generates the spectacular colossal magneto-resistance effect (CMR). The coexistence of the ferromagnetic state and metallicity has been explained using the double exchange (DE) mechanism, related to mobile e_g electrons traveling between the Mn^{3+} and Mn^{4+} cations as proposed by Zener [5,6]. This model confirmed that the ferromagnetic spin correlation is the characteristic feature of in the paramagnetic state.

Recent investigations have demonstrated that the varying doping level x in A-site plays important role in modification of magnetic and transport properties of the manganites. Hwang et al. [7] showed a direct relationship between the average ionic radius for the A-site ion $<r_A>$ and the Curie temperature T_C in the substituted manganites $Ln_{1-x}Sr_xMnO_3$ for $x = 0.3$. Recently the studies on monovalent doped manganites (e.g. Na, K) are attracting the attention, because it allows to achieve the same amount of hole doping with a half substitution. Among the most studied monovalent doped manganites, sodium doped lanthanum manganites are found to exhibit large negative magnetoresistance (MR) at room temperature and do not show charge ordering for $0 < x < 0.40$ [8], which simplifies analysis of results. This feature is in contrast to the Na doped Pr based manganites $Pr_{1-x}Na_xMnO_3$, which have been reported to exhibit charge ordering behavior for $0.2 < x < 0.25$ [9,10].

The electron magnetic resonance (EMR) is applied since it offers a sensitive experimental technique to understand the dynamics of the electronic spins, and can help to clarify the magnetic correlation on a microscopic level in mixed valency manganites [11]. Our paper supplements previous studies of Pr/Sr based manganites [12] and is aimed at deeper investigation of the influence of monovalent sodium co-doping on properties of polycrystalline $Pr_{0.6}Sr_{0.4}MnO_3$ manganite. There have been no previous EMR studies on the Na-doping effect in the $Pr_{0.6}Sr_{0.4}MnO_3$ system. In this work we focus on the substitution of monovalent Na for Sr in the $Pr_{0.6}Sr_{0.4}MnO_3$ manganites studied using EMR spectroscopy. Temperature dependence of resonance line width and intensity are analyzed by means of the small polaron hopping model.

2. Experimental

Polycrystalline samples of the undoped $Pr_{0.6}Sr_{0.4}MnO_3$ (PS) manganite and sodium doped $Pr_{0.6}Sr_{0.35}Na_{0.05}MnO_3$ (PSN) one were synthesized from high purity

* Corresponding author. Tel.: +216 98974687; fax: +216 74676607.
E-mail address: Wahibaboujelben@yahoo.fr (W. Boujelben).

0925-8388/$ – see front matter © 2012 Elsevier B.V. All rights reserved.
doi:10.1016/j.jallcom.2012.02.096

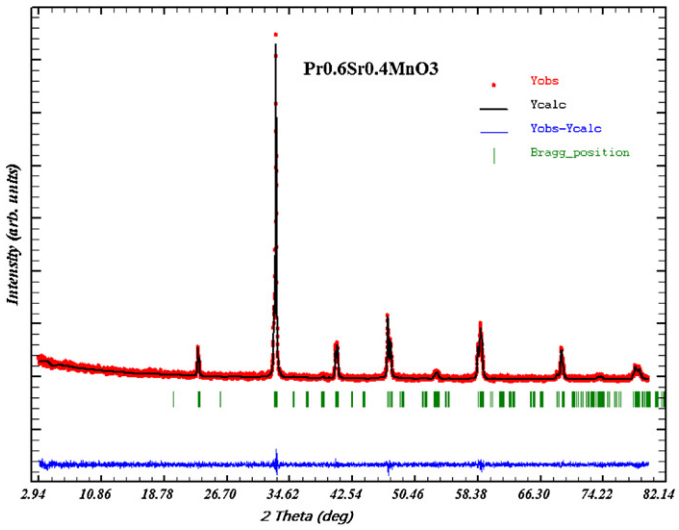

Fig. 1. XRD diffraction pattern for the undoped $Pr_{0.6}Sr_{0.4}MnO_3$ (PS) manganite.

(>99.9%) Pr_6O_{11}, $SrCO_3$, Na_2CO_3 and MnO_2 by conventional solid state reaction method. The starting materials were initially mixed in an agate mortar and then heated in air up to 900 °C for 60 h. The obtained powders were then pressed into pellets and sintered at 1100 °C in air for 60 h with intermediate regrinding and repelling. Finally, these pellets were quenched to room temperature in air in order to freeze the structure at the annealed temperature. Phase purity, homogeneity and cell dimensions were determined by powder X-ray diffraction at room temperature. As our samples have been synthesized in air, they are stoichiometric in oxygen [13]. Structural analysis was made using the standard Rietveld technique [14,15] and a typical plot of the refined pattern is shown in Fig. 1 for (PS) sample proves that the main peaks can be indexed to the single orthorhombic perovskite structure with *Pnma* space group. Structural analysis of the doped sample was described separately in previous work [16]. We should note that for 0.05 Na content no apparent structural changes can be identified. The unit cell volume decreases slightly from 229.108 Å^3 for parent sample to 228.76 Å^3 for doped sample, which can be explained by a smaller average ionic radius of Na^+ (1.39 Å) than Sr^{2+} (1.44 Å) one [17]. The polycrystalline structure is rather fine with mean crystallite size about 41 nm for (PS) and 32 nm for (PSN). The magnetic characterization was carried out using a vibrating sample magnetometer and shows that Na doping shifts the ferromagnetic Curie temperature from 310 K to 300 K (Fig. 2). Electron magnetic resonance measurements were performed with loose powder in a capillary using a Bruker spectrometer, operating at 9.44 GHz (X-band) between 130 and 375 K. Calibration was carefully performed using DPPH standard.

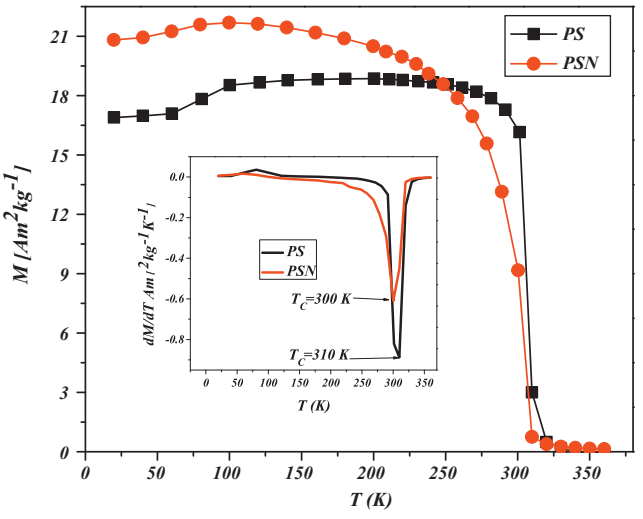

Fig. 2. Temperature variation of magnetization measured at magnetic field of 0.05 T for the undoped $Pr_{0.6}Sr_{0.4}MnO_3$ (PS) and Na doped $Pr_{0.6}Sr_{0.35}Na_{0.05}MnO_3$ (PSN) manganites.

3. Analysis of EMR spectra

In manganites the EMR signal is related to the combination of Mn^{3+}–Mn^{4+} ions coupled by strong short range FM double exchange interaction [18,19]. The EMR spectra of the undoped (PS) (Fig. 3a) and Na doped (PSN) (Fig. 3b) manganites recorded in a broad temperature range change remarkably at transition from paramagnetic to ferromagnetic phase. In the paramagnetic phase the EMR consists of a single symmetrical Lorentzian line. For the temperature decreasing through the transition temperature T_C from paramagnetic to ferromagnetic phase the signal broadens and becomes asymmetric revealing a superposition of paramagnetic and ferromagnetic components. A fraction of paramagnetic signal is quickly decaying with decreasing temperature.

The EMR measurements are analyzed in a standard manner [11]. The resonance field H_{res} was determined with accuracy ±4 Oe. The line width ΔH is taken from the peak-to-peak distance between the maximum and the minimum of the first derivative of the EMR absorption signal. The asymmetry is defined by the maximum to minimum ratio. The intensity of the response is defined by $A(\Delta H)^2$, where A is the peak to peak amplitude. The g_{eff} value is calculated via $g_{eff} = h\upsilon/\mu_B H_{res}$, where h is the Planck constant, μ_B is the Bohr magneton, υ is the frequency and H_{res} is the resonance field. Accuracy of g_{eff} is about ±0.0025.

The registered spectra exhibit a maximum amplitude A at 315 K and 305 K for the PS and PSN manganites, respectively, which are close to their Curie temperatures T_C = 310 K and 300 K, respectively, as determined from magnetization measurements. It is observed (not plotted) that the signal amplitude decreases quickly both below and above the Curie temperature for our investigated samples. The coexistence of competing ferromagnetic and paramagnetic resonance signals found in vicinity of Curie temperature reveals a phase coexistence in the samples.

The resonance field (H_{res}) decreases slowly in the paramagnetic phase from 3366 Oe at 370 K down to 3299 at 315 K for undoped PS sample and from 3360 Oe at 375 K down to 3300 Oe at 305 K for doped PSN sample (Fig. 4). These fields correspond to g_{eff} values of 2.0126 and 2.0370 for doped manganite, and 2.0085 and 2.0364 for undoped manganite. The g_{eff} values are typical for the electron response for doped manganite in the paramagnetic state [11,20]. It is worth noticing that in the high temperature range the g_{eff} values obtained from H_{res} exhibits a weak temperature dependence. This observation confirms that the spin–spin interaction between Mn^{3+} and Mn^{4+} ions dominates in the paramagnetic region.

The EMR line width ΔH is a non monotonic function of temperature as shown in Fig. 5 for a broad temperature interval. This plot shows the characteristic ΔH minimum at T_{min} equal to 330 K and 315 K for the undoped and doped manganites, respectively, located slightly above the corresponding Curie temperatures. Such a location of ΔH minimum somewhat above T_C is typical for manganites and was also reported for other manganites, e.g. $La_{1-x}Sr_xMnO_3$ [21,22]. The minimum line width equals to 275 Oe and 255 Oe for the undoped and doped manganites, respectively. The minimum line width corresponds to the transverse relaxation time about 0.5 ns, giving spin exchange narrowing which is typically reported for manganites [23]. In the ferromagnetic phase the line width ΔH abruptly raises up to about 3 kOe at 130 K and 4 kOe at 200 K for the undoped and doped manganites, respectively (Fig. 3). This line width broadening observed at low temperature is usually ascribed to the slowing down of spin fluctuations in the ferromagnetic phase. The increasing of the line width observed between T_C and T_{min} can be related to the coexistence of the ferro- and paramagnetic phases. In the paramagnetic phase the minimum is followed by a slow increase up to 445 Oe at 370 K and 541 Oe at 375 K respectively for undoped (PS) and doped (PSN) samples. In this temperature range the mean slope ($d(\Delta H)/dT$) is equals to 5.2 and 5.9 Oe/K

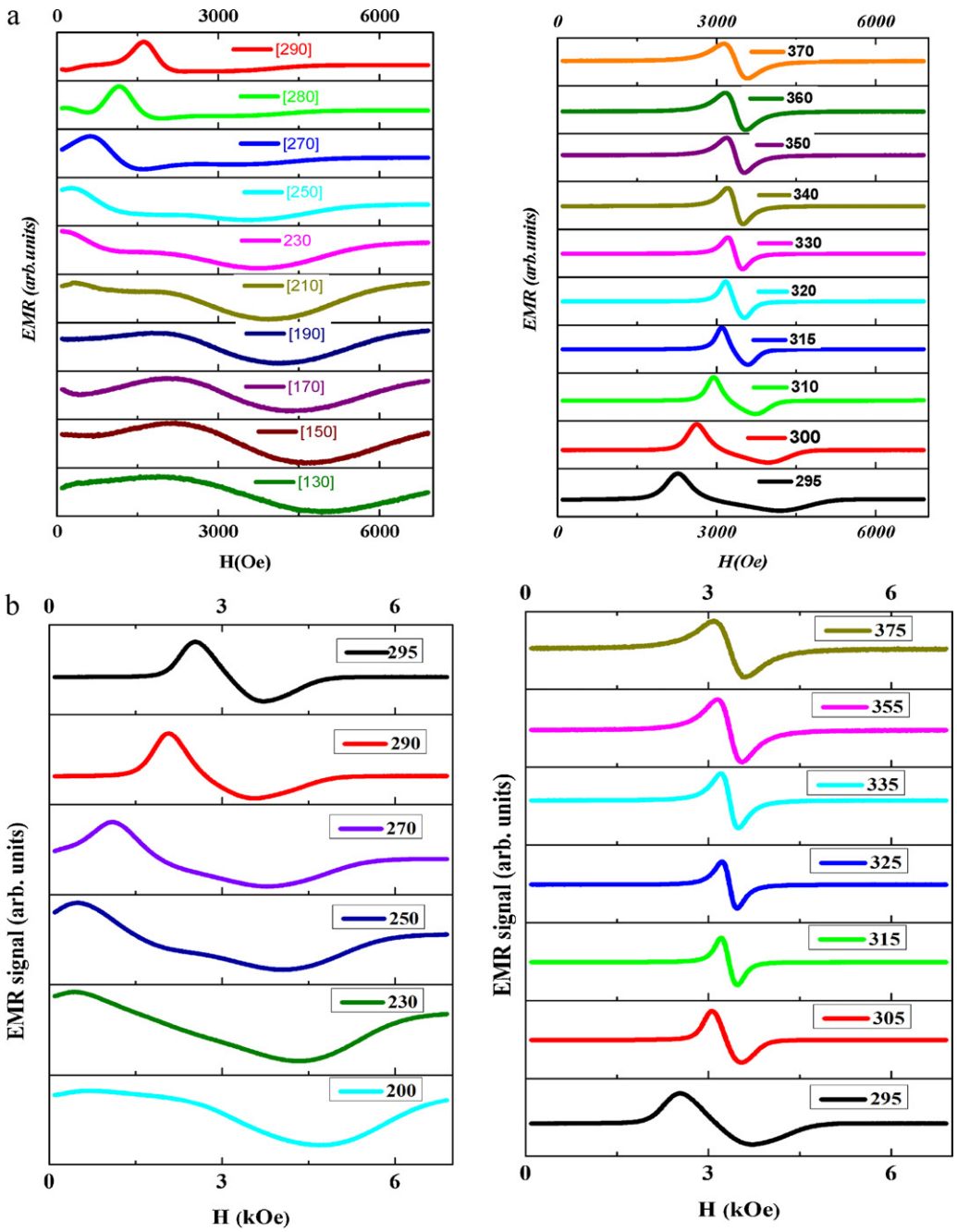

Fig. 3. (a) Electron magnetic resonance spectra of the undoped $Pr_{0.6}Sr_{0.4}MnO_3$ (PS) manganite. (b) Electron magnetic resonance spectra of the Na doped $Pr_{0.6}Sr_{0.35}Na_{0.05}MnO_3$ (PSN) manganite.

respectively for PS and PSN samples. These results are comparable to that reported for similar manganites [24,25]. The single and relatively broad ΔH minimum is related to the Jahn–Teller transition [26], which develops the long range ordering at low temperature.

The deeper examination of temperature variation of ΔH enables to determine the activation energy, when assuming a model of adiabatic small polaron hopping [18], which expresses the signal width by the following expression:

$$\Delta H(T) = \Delta H_0 + \left(\frac{A}{T}\right) \exp\left(\frac{-E_1}{kT}\right) \quad (1)$$

where ΔH_0 is constant. The activation energy E_1 derived from an inset to Fig. 5 equals to 162 and 188 meV for the doped and undoped samples, respectively. The results obtained from the best fitting show that the activation energy slightly decrease with Na-doping.

Temperature variation of signal intensity $I(T)$ for our samples is shown in Fig. 6. One should notice that the accuracy of applied $I(T)$ calculation is high enough only in paramagnetic phase, where signals are approximately symmetric (Fig. 7). The same calculation method used below 295 K results in much reduced accuracy since the EMR signals become strongly asymmetric in the ferromagnetic phase, as indicated by the asymmetry factor deviating much from 1. Therefore the $I(T)$ dependence below T_C offers only rough approximation and shows that intensity raises abruptly with temperature varying down to 130 K (not plotted). The similar intensity variation was already reported for e.g. $Pr_{0.7}Sr_{0.3-x}Ba_xMnO_3$ manganite [27]. Taking as a reference the intensity at Curie temperature one can see that in the paramagnetic phase the intensity decreases just above T_C and then more slowly with temperature raising up to 375 K.

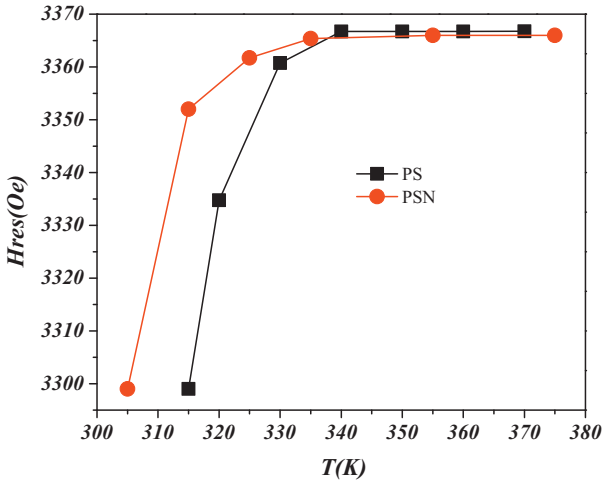

Fig. 4. Temperature variation of magnetic resonance field for the PS and PSN manganites.

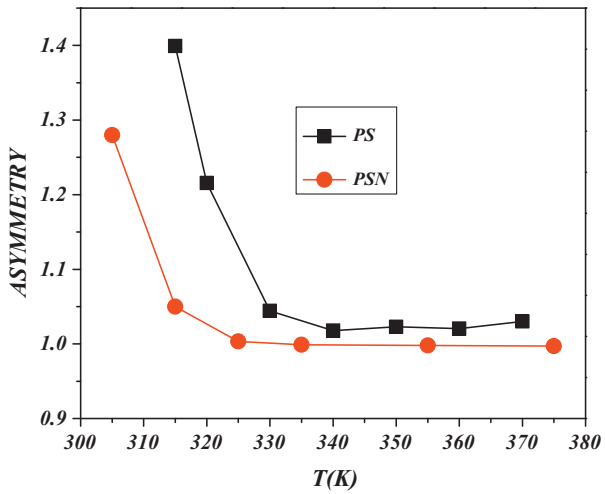

Fig. 7. Temperature variation of signal asymmetry for the PS and PSN manganites.

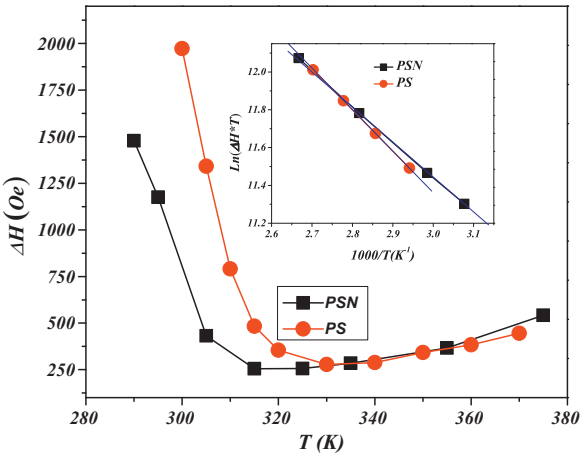

Fig. 5. Temperature variation of peak to peak line width for the PS and PSN manganites. Inset shows Ln ($\Delta H * T$) vs (1000/T).

The signal intensity $I(T)$ is proportional to magnetic susceptibility of the material, which in the paramagnetic state is expected to follow the Curie–Weiss law. The inverse intensity as a function of temperature for undoped and doped samples is plotted in Fig. 8. The linear variation observed at higher temperatures, shows that the Curie–Weiss law is obeyed for both manganites, whereas deviations appear below about 315 K and 305 K for undoped (PS) and doped (PSN) manganites, respectively. The so-called paramagnetic Curie (Weiss) temperature T_P derived by extrapolation of linear dependence is equals to 312 K and 306 K, respectively for (PS) and (PSN) samples. These paramagnetic Curie temperature are close to values derived from inverse magnetization measured at magnetic field of 0.05 T (Fig. 2), which are equal to 316 and 298 K for undoped and doped manganites, respectively. The higher Curie temperature of the undoped than doped manganite shows that the magnetic interaction in paramagnetic phase becomes weaker in doped sample. It is worth noticing that also below the magnetic phase transition the ferromagnetic interaction in sodium doped manganite is weaker as compared to undoped case, as it is revealed by a ratio of ferromagnetic Curie temperatures (310 and 300 K) derived from magnetization. A magnitude of double exchange interaction in magnanites is known to depend on Mn–O–Mn angle. The structural data show that the angle is changed negligibly from

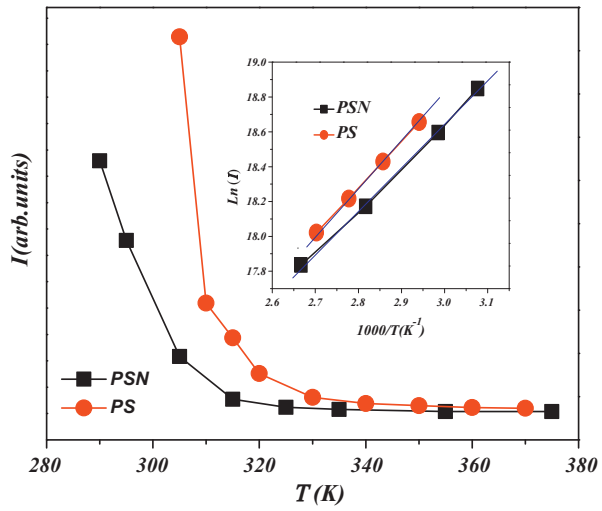

Fig. 6. Temperature variation of signal intensity for the PS and PSN manganites. Inset shows Ln (I) vs (1000/T).

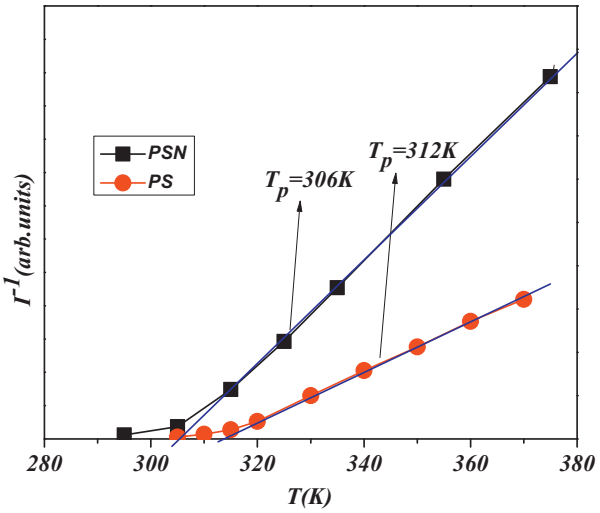

Fig. 8. Temperature variation of the inverse signal intensity for the PS and PSN manganites.

161.96(1)° to 161.26(1)° when passing from undoped to doped manganites.

The resonance spectra were recorded in identical experimental condition for both the manganites. Therefore the absolute values of inverse intensity values are close in vicinity of 310 K (Fig. 8). Then one may compare the slopes of inverse intensity vs temperature, which are proportional to inverse Curie constant. As the Curie constant is proportional to the square of effective magnetic moment one may qualitatively estimate that Na doping into A-sites suppresses the effective magnetic moment. This is at least partially due to the fact that 5% of sodium replacing Sr atoms changes the Mn^{3+}/Mn^{4+} ratio from 0.6/0.4 to 0.55/0.45. Moreover, the sodium doping enhances local disorder and reduces double exchange integral [5,6].

The temperature variation of signal intensity in paramagnetic state may be expressed as follows:

$$I(T) = I_0 \exp\left(\frac{E_2}{k_B T}\right) \quad (2)$$

where k_B is the Boltzmann constant and E_2 is the activation energy of electron hopping [19]. The straight line fitted to the experimental intensity (Fig. 6 inset) confirms that this relation is obeyed with E_2 equal to 213 and 230 meV, for doped and undoped samples, respectively. Such activation energies are somewhat larger than those derived from line width. A difference in activation energy derived from line width and line intensity are not unusual. Similar order of magnitude and ratio of energies was also reported for the Sr doped and other manganites [22–25]. A comparison of activation energies derived both from the intensity and line width data confirms that the Na doping hampers hopping phenomena as indicated by the higher values found for the doped sample. The thermally activated behavior of magnetic susceptibility reveals that the polaron hopping reduces the spin correlations in paramagnetic phase [19].

4. Conclusions

These experimental results evidently show that the paramagnetic and ferromagnetic phases coexist in the $Pr_{0.6}Sr_{0.4-x}Na_xMnO_3$ ($x = 0, 0.05$). The growing ferromagnetic phase creates an internal magnetic field which in turn makes smaller the registered resonance field of the EMR signals as well as modifies the signal shape. Applying cautiously an analogy to related manganites [28] one may also speculate that the ferromagnetic phase forms mainly inside the relatively small crystallites with mean size of 32 and 41 nm, whereas the structurally more disordered paramagnetic phase prevails at the surface of grains/crystallites.

Acknowledgements

This work was supported by the Tunisian Ministry of Higher Education and Scientific Research and the Ministry of Science and Higher Education of Poland.

References

[1] C.N.R. Rao, B. Raveau (Eds.), Colossal Magnetoresistance Charge Ordering and Related Properties of Manganese Oxides, World Scientific Singapore, 1998.
[2] Y. Tokura, Colossal Magnetoresistance Oxides, Gordon and Breach, New York, 2000.
[3] T. Venkatesan, M. Rajeswari, Z.-W. Dong, S.B. Ogale, R. Ramesh, Philos. Trans. R. Soc. Lond. Ser. A 356 (1998) 1661.
[4] A.M. Haghiri-Gosnet, J.-P. Renard, J. Phys. D: Appl. Phys. 36 (2003) R127.
[5] C. Zener, Phys. Rev. 82 (1951) 403.
[6] P.G. de Gennes, Phys. Rev. 118 (1960) 141.
[7] H.Y. Hwang, S.W. Cheong, M.M. Radaelli, B. Batlogg, Phys. Rev. Lett. 75 (1995) 914.
[8] S. Roy, Y.Q. Guo, S. Venkatesh, N. Ali, J. Phys.: Condens. Matter 13 (2001) 9547.
[9] J. Hejtmanek, Z. Jirak, J. Sebek, A. Strejc, J. Appl. Phys. 89 (2001) 7413.
[10] D.P. Kozlenko, Z. Jirak, I.N. Goncharenko, B.N. Savenko, J. Phys.: Condens. Matter 16 (2004) 5883.
[11] C. Autret, M. Gervais, F. Gervais, N. Raimboux, P. Simon, Solid State Sci. 6 (2004) 815.
[12] P. Pal, M.K. Dalai, B.R. Sekhar, S.N. Jha, S.V.N. Bhaskara Rao, N.C. Das, C. Martin, F. Studer, J. Phys.: Condens. Matter 17 (2005) 2993.
[13] J.H. Kuo, H.U. Anderson, D.M. Sparlin, J. Solid State Chem. 83 (1989) 52.
[14] H.M. Rietveld, J. Appl. Crystallogr. 2 (1969) 65.
[15] T. Roisnel, J. Rodriguez-Carvajal, Computer Program FULLPROF, LLB-LCSIM, May 2003.
[16] R. Thaljaoui, J. Alloys.compd., submitted for publication.
[17] R.D. Shanon, Acta Crystallogr. A 32 (1976) 751.
[18] A. Shengelaya, G.M. Zhao, H. Keller, K.A. Muller, Phys. Rev. Lett. 77 (1996) 5296.
[19] S.B. Oseroff, M. Torikachvili, J. Singley, S. Ali, S.W. Cheong, S. Schultz, Phys. Rev. B 53 (1996) 652.
[20] J. Gutierrez, V. Siruguri, J.M. Barandiaran, A. Pena, L. Lezama, T. Rojo, Physica B 372 (2006) 173.
[21] A.I. Shames, E. Rozenberg, M. Auslender, D. Mogilyansky, E. Sominski, A. Gedanken, Solid State Commun. 151 (2011) 1593.
[22] T.L. Phan, N.D. Tho, L.V. Bau, N.X. Phuc, S.C. Yu, J. Magn. Magn. Mater. 303 (2006) e339.
[23] V.A. Atsarkin, V.V. Demidov, G.A. Vasneva, D.G. Gotovtsev, Appl. Magn. Res. 21 (2001) 147.
[24] A.N. Ulyanov, S.C. Yu, S.G. Min, G.G. Levchenko, J. Appl. Phys. 91 (2002) 7926.
[25] C. Rettori, D. Rao, J. Singley, D. Kidwell, S.B. Oseroff, M.T. Causa, J.J. Neumeier, K.J. McClellan, S.-W. Cheng, S. Schulz, Phys. Rev. B 55 (1997) 3083.
[26] G. Alejandro, M.C.G. Passeggi, D. Vega, C.A. Ramos, M.T. Causa, M. Tova, R. Senis, Phys. Rev. 68 (2003) 214429.
[27] P.H. Quang, Y.S. Chang, A.N. Ulyanov, N.E. Pismenova, S.C. Yu, Phys. Stat. Sol. B 241 (2004) 1569.
[28] A.I. Shames, M. Auslender, E. Rozenberg, E. Sominski, A. Gedanken, Ya.M. Mukovskii, J. Appl. Phys. 103 (2008) 07F715.